Influence of Neutron Irradiation on the Large Helical Device Thomson Scattering System*)

Ichihiro YAMADA, Hisamichi FUNABA, Jong-ha LEE[1)], Yuan HUANG[2)] and Chunhua LIU[2)]

National Institute for Fusion Science, Toki 509-5292, Japan
[1)]*National Fusion Research Institute, Daejeon 34133, Korea*
[2)]*Southwestern Institute of Physics, P.O. Box 432, Chengdu 610041, China*

(Received 2 January 2020 / Accepted 19 August 2020)

Since 2017, deuterium plasma experiments (DD experiments) have been performed in large helical device (LHD), where neutrons with a specific energy of 2.45 MeV are generated through deuterium thermonuclear fusion reactions, and the influence on the devices located near the LHD are concerned. For the LHD Thomson scattering system, a view window, a light collection mirror, and optical fibers have been installed near the LHD. Degradation by neutron irradiation may cause serious problems in the results from the Thomson scattering diagnostic. We discuss the calibration of the three components and the neutron influences on the LHD Thomson scattering diagnostics.

Keywords: Thomson scattering diagnostic, large helical device, calibration

DOI: 10.1585/pfr.15.2402075

1. Introduction

The large helical device (LHD) Thomson scattering (TS) system has measured electron temperature and density profiles of LHD plasmas since 1998 [1–3]. In LHD, deuterium plasma experiments (DD experiments) have been performed since 2017. In the DD experiments, 2.45 MeV neutrons are generated through DD fusion reactions. Neutrons can easily transmit from the LHD vacuum vessel inside to the outside, so the effect on the devices located near LHD are concerned. For the LHD TS system, there is a view window, a light collection mirror, and optical fibers near LHD. If changes in window transmittance, fiber transmittance, and mirror reflectance occur, they can cause problems with the results from the TS diagnostic. In the design and development of the LHD TS system in 1991-1997, we carefully determined the component materials for the components based on the literature and discussions with some optical component manufactures [4–7]. It is difficult to remove the view window, light collection mirror, and optical fibers out from the LHD hall, so in situ calibrations are necessary. In section 2, we discuss the calibration of the three components. The calibration for the other components of the LHD TS is summarized in previous literature [8]. Next, section 3 describes the newly developed neutron effect monitoring system for the fibers.

2. Calibration

2.1 Calibration of the view window

The LHD TS view window is made from fused silica. The dimensions are 60 cm wide × 35 cm high × 5 cm thick. In addition to the view window, there is an additional protection glass inside the LHD vacuum vessel. This protection glass was installed to protect the main window against high-energy particles and strong radiation escaping from plasmas. The thickness is 1 cm. Both of two glasses do not have an anti-reflection coating, so there is a Fresnel reflection loss of ∼16%. We performed the calibration of the wavelength dependence of the (window + protection glass) transmittance.

Figure 1 shows a schematic diagram of the calibration setup. First, we put a flat Al mirror inside the vacuum vessel. Next, a light beam is injected toward the Al mirror from the outside, and the spectrum of the reflected light is measured with a spectrometer (Hamamatsu, C9405CB). The probe light is generated with a halogen lamp (Avantes, AvaLight HAL-S-MINI) and collimated with a fiber light collimator consisting a triplet lens (Techno Synergy, BBFC02-SMA). The spot diameter of the light beam emitted from the collimator is approximately 5 - 20 mm (adjustable) at the position between 20 cm and 100 cm. The reflectance of the flat Al mirror alone is measured in a laboratory. The relative transmittance of the (window + protection glass) is obtained from the ratio of the measured spectrum of (window + protection glass + Al mirror) and Al mirror. Also, a similar measurement was performed using a HeNe laser with a diameter of less than 1 mm (Tholabs, HNL050RB) and a Si-photodetector with a diameter of 9.7 mm (Tholabs, PDA100A2) at 633 nm to obtain absolute transmittance. Absolute transmittance is determined by normalizing the relative transmittance, measured by the spectrometer, to

author's e-mail: yamadai@nifs.ac.jp
*) This article is based on the presentation at the 28th International Toki Conference on Plasma and Fusion Research (ITC28).

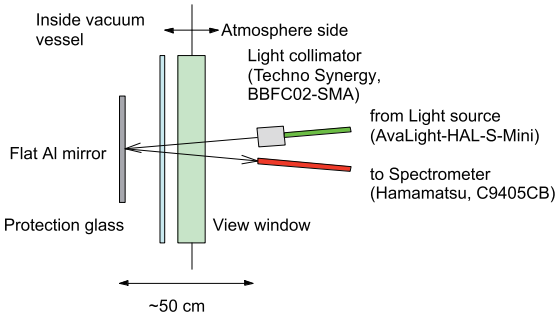

Fig. 1 Schematic diagram of the window transmittance calibration.

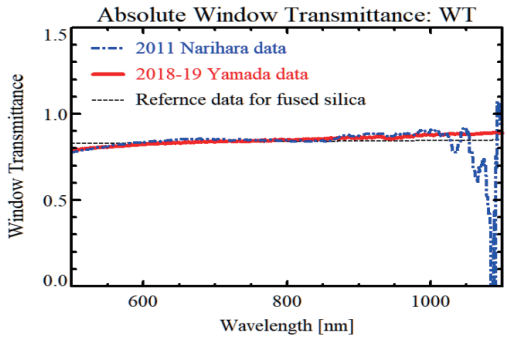

Fig. 2 Window transmittance. Solid and dotted curves show the current result (2018-19) and one obtained from the previous measurement (2011), respectively.

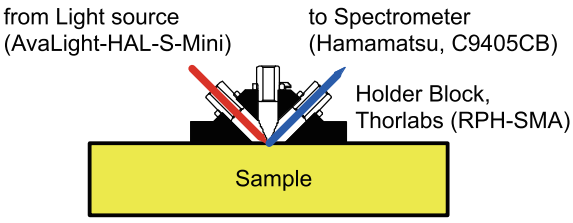

Fig. 3 Schematic diagram of the mirror reflectance calibration. In this study, the 45 degree reflected light for 45 degree incidence –45 degree reflection is observed.

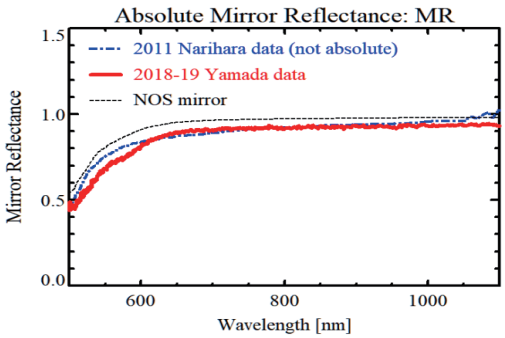

Fig. 4 Absolute mirror reflectance. Solid and dotted curves show the current data (2018-19) and previous data (2011), respectively. Dashed curve shows measured reflection for a new old stock (NOS) mirror.

HeNe data at 633 nm. Figure 2 compared the current result with a previous one measured in 2011. Because the sensitivity of the spectrometer used in the previous measurement rapidly decreased above 1000 nm, the previous result's reliability is poor above 1000 nm. The two results show good agreement between 500 and 1000 nm.

2.2 Calibration of the light collection mirror

In order to collect weak TS light, we use a large, gold-coated mirror. The mirror consists of small 138 hexagonal mirrors, and the total dimensions are 1.5-m width and 1.8-m high. Similar to the window transmittance calibration, we measured the relative reflectance of 39 of 138 mirrors by using a halogen light, a spectrometer, and a holder block for fiber optic probes (Tholabs, RPH-SMA). This tool is useful for measuring the reflectance of solid, liquid, and powder samples, as shown in Fig. 3. In this calibration, we measure the reflectance for the 45-degree incidence – 45-degree reflection configuration. We assumed that the reflectance of flat, clean mirrors have no (or negligibly small) angular dependence. In the preliminary test, we confirmed that there is no difference between the reflectance for 45-degree incidence – 45-degree reflection and the 0-degree incidence – 0-degree reflection. Absolute reflectance is determined by using a reference new gold mirror whose absolute reflectance data is provided by the manufacturer (Shigma-koki). Figure 4 shows the result of the absolute reflectance of the light collection mirror with previous measurement in 2011. The result of a new old stock (NOS) mirror is also plotted. When comparing to the NOS mirror, a clear degradation owing to contamination is seen, i.e., −7%, −5%, and −5% at 633, 800, and 1000 nm, respectively. From visual inspection, some mirrors are clearly dirty, and some mirrors are still relatively clean. In the figure, the averaged value of 39 mirrors is plotted. The deviation for 39 mirrors is 7%. To check the reliability of the data, we also performed absolute measurements of the mirror reflectance at 633 nm by using a HeNe laser and a Si-photodetector similar to the window transmittance measurement. The two absolute reflectances show good agreement measured at 633 nm within the experimental error (3%).

2.3 Calibration of the optical fiber

In the LHD TS system, TS light is transferred to polychromators through optical fibers whose core diameter and length are 2.0 mm and 45 m, respectively. Both the core and clad of the fiber are made of pure anhydrous, synthetic quartz of which OH concentration is less than several ppm without any specific dopant. Figure 5 shows the schematic diagram of the measurement of the optical fiber transmittance. The path #1 consists of two 42-m fibers and one 12-m fiber. Thus, the total path length is 96 m. The path

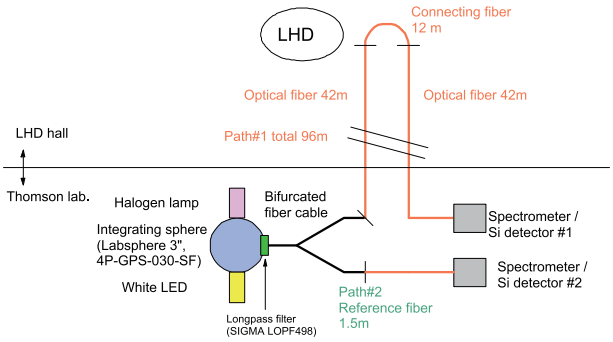

Fig. 5 Schematic diagram of the fiber transmittance calibration. Path #2 is a reference path.

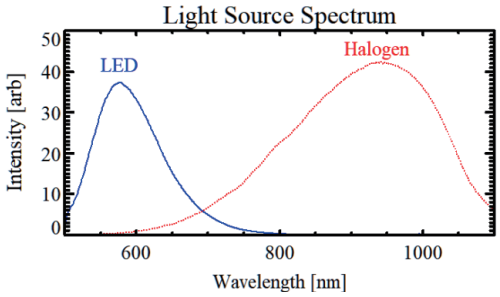

Fig. 6 Light source spectrum used in this study. Halogen and LED lights are used for the measurements in longer and shorter wavelength regions, respectively.

#2 is used for the reference path. The length is 1.5 m. As light sources, we used a halogen and LED lamps, for longer wavelength and shorter wavelength regions, respectively. Figure 6 shows the light source spectrum. The right and left peaks are generated by a halogen lamp and LED lamp, respectively. The two lights are mixed with an integrating sphere (Labshere, 4P-GPS-030-SF), and the output is transferred to the entrances of paths #1 and #2 through a bifurcated fiber (Avantes, 1FC-UVIR400-2). A spectrometer or silicon photodiode observed transmitted light through paths #1 and #2. Transmittance, t_x, is expressed by the attenuation equation, $t_x = \exp(-ax)$, where a is the attenuation coefficient, and x is the fiber length. From the measured data for paths #1 and #2, we can determine the attenuation coefficient, a, Fresnel loss, F, and connection loss, C, at the injections. In this calibration, we assumed that a, F, and C is the same for all fibers. The results for Fresnel loss and connection loss are estimated to be 3.3% and 4.9%, respectively. The theoretical value of F is 3.5%, and the connection loss is considered to be less than 6% from the model calculation. Thus, both of them are reasonable. Figure 7 shows the fiber transmittance measured in this work with the previous measurement in 2011, and data provided from the manufacturer. The data are in good agreement except for the previous data above 1000 nm. As discussed in section 2.1, the reliability of the previous result is poor above 1000 nm because the sensitivity of the

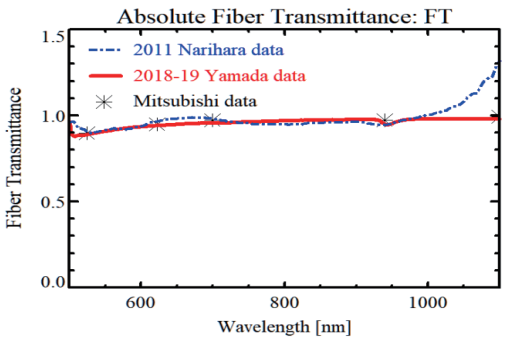

Fig. 7 Solid and dotted curves show the present result (2018-19) and previous measurement (2011), respectively. Data provided by the fiber manufacturer (Mitsubishi) are also plotted (stars).

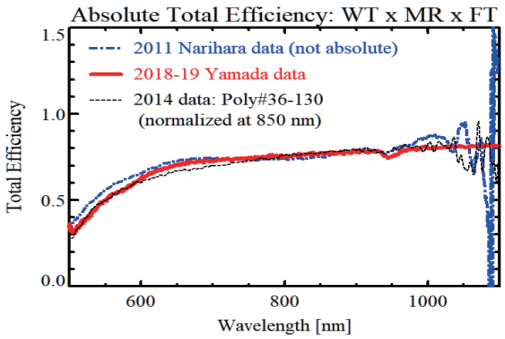

Fig. 8 Comparison of the total efficiencies measured in 2011, 2014, and 2018-19.

spectrometer used in the previous measurement is poor.

2.4 Comparison of overall efficiency

We measured the overall light transmittance in 2014. A light source was set inside the LHD vacuum vessel, and the spectrum of the transmitted light was observed by a spectrometer. In this calibration, the overall coefficient, i.e., the product of window transmittance × mirror reflectance × fiber transmittance, is obtained. We compared the product of three elements obtained in this calibration with the previous result as shown in Fig. 8. Because the previous result was a relative calibration, it is normalized to the current result at 850 nm. These results are in a very good agreement between 500 nm and 1000 nm, which shows that both of the measurements in 2014 and 2018-9 are reliable.

3. Neutron Effect Monitoring System for the Optical Fiber

The total amount of neutrons generated in the 2019 LHD DD experiment was 0.34×10^{19}. In LHD DD experiments, the gross maximum neutron generation is estimated to be 1.9×10^{16} neutrons/s. The maximum neutron flux for the fibers is estimated to be $\sim 1 \times 10^{14}$ neutrons/m^2/s. The

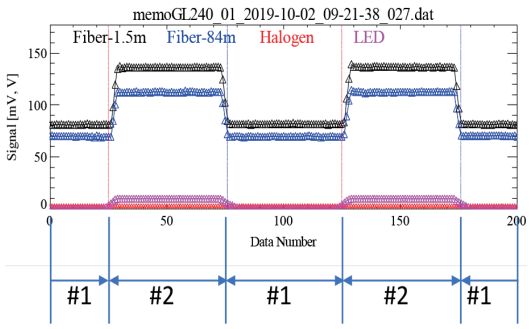

Fig. 9 Signal intensity detected by Si detectors. In the phase #1, only the halogen lamp is on. Both the halogen and LED lamps are lit in the phase #2.

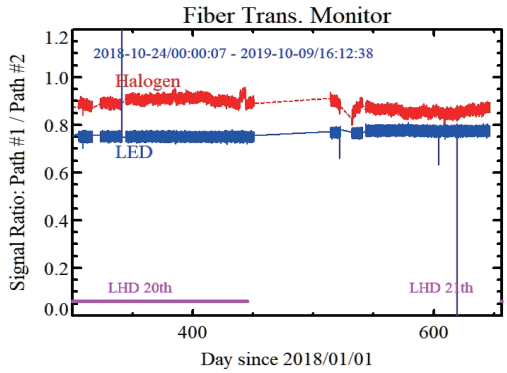

Fig. 10 Signal intensity ratios of the path #1/path #2 for halogen lamp (upper) and LED lamp (lower). No clear temporal change is seen up to now.

gamma-ray intensity is estimated to be ~1/10 that of neutrons.

Of the three components discussed in the previous section, the optical fiber is considered to be most affected by neutron irradiation because the light transmission length is much longer (45 m) than the thickness of the window (5 cm). Therefore, we developed an optical fiber transmission monitoring system. The schematic diagram is almost the same as that used in the fiber calibration. In this system, we connected two 42-m fibers without using a connection fiber of 12 m to simplify the path. Thus, the total path length of the path #1 is 84 m. The fibers in the path #1 pass near the LHD, where strong neutron irradiation is expected. On the other hand, the path #2 is located in a laboratory that is sufficiently radiation-shielded, and the length is considerably shorter than that of the path #1. Therefore, we can assume that the neutron effect does not occur in the path #2.

In the system, the LED light is modulated at the frequency of 0.2 Hz, as shown in Fig. 9, whereas the halogen lamp is always on. In the phase #1, only the halogen lamp is on, and transmittance for relatively long wavelength is observed. In the phase #2, both the halogen and LED lamps are on. By subtracting the signal intensity at the phase #1 from that at the phase #2, the signal intensity for the LED lamp is obtained. We have been observing the signal intensities for the paths #1 and #2 since 2018. Figure 10 shows the light intensity ratio of the paths #2 and #1. It is noted that the data is missing between 450 and 520 days, because we performed improvements and tests these days. The signal intensity ratio was slightly changed due to the improvement work. Currently, no significant changes are observed. We are planning to continue this measurement to verify the reliability of the TS data.

4. Summary

Since 2017, deuterium plasma experiments (DD experiments) have been performed in LHD. For the three components of the LHD TS system, neutron irradiation can degrade a view window, a light collection mirror, and optical fibers. We performed new calibrations for the three components, and obtained more reliable calibration data than previous ones. Specially, we developed a new fiber transmittance monitoring system for optical fibers that are expected to be most affected by neutron irradiation. Up to now, no significant neutron effect has been observed. This result will be useful for future fusion plasma diagnostic research.

Acknowledgements

This work was supported by the NIFS budget, ULHH005 and JSPS KAKENHI, 18K03586.

[1] K. Narihara *et al.*, Fusion Sci. Des. **34-35**, 67 (1997).
[2] K. Narihara *et al.*, Rev. Sci. Instrum. **72**, 1122 (2001).
[3] I. Yamada *et al.*, Fusion Sci. Des. **58**, 345 (2010).
[4] P.D. Morgan *et al.*, Rev. Sci. Instrum. **56**, 862 (1985).
[5] A.T. Ramsey *et al.*, Rev. Sci. Instrum. **63**, 4735 (1992).
[6] W. Tighe *et al.*, Rev. Sci. Instrum. **66**, 907 (1995).
[7] A.T. Ramsey *et al.*, Rev. Sci. Instrum. **68**, 632 (1997).
[8] I. Yamada *et al.*, Rev. Sci. Instrum. **87**, 11E531 (2016).